Biosensors and Bioelectronics 26 (2010) 1080–1086

Contents lists available at ScienceDirect

Biosensors and Bioelectronics

journal homepage: www.elsevier.com/locate/bios

A selective nitric oxide nanocomposite biosensor based on direct electron transfer of microperoxidase: Removal of interferences by co-immobilized enzymes

Adel A. Abdelwahab, Wei Choon Alvin Koh, Hui-Bog Noh, Yoon-Bo Shim *

Department of Chemistry and Institute of BioPhysio Sensor Technology, Pusan National University, Busan 609-735, South Korea

ARTICLE INFO

Article history:
Received 5 July 2010
Received in revised form 17 August 2010
Accepted 20 August 2010
Available online 22 September 2010

Keywords:
Cancer cells
Catalase
Microperoxidase
Nitric oxide biosensor
Rat liver
Superoxide dismutase

ABSTRACT

A highly selective nitric oxide (NO) biosensor was developed by immobilizing microperoxidase (MP) onto the MWCNT-poly-5,2′:5′,2″-terthiophene-3′-carboxylic acid (PTTCA) nanocomposite. Catalase (CAS) and superoxide dismutase (SOD) co-immobilized on the probe successfully protected the interferences of H_2O_2 and O_2^- during NO detection. The nanocomposite layer showed the direct electron transfer processes of the immobilized CAS, SOD, and MP simultaneously at −0.11/+0.04, −0.33/−0.27, and −0.47/−0.40 V vs. Ag/AgCl. Au nanoparticles (AuNPs) were electrodeposited on a glassy carbon surface to enhance the sensitivity of the sensor probe. The layers of CAS/SOD/MP/MWCNT-PTTCA/AuNPs were characterized using SEM, XPS, and QCM. The CAS/SOD/MP/MWCNT-PTTCA/AuNPs probe showed an excellent performance in the electrocatalytic reduction of NO which was attributed to the heme group of MP. Experimental conditions affecting the sensitivity of the biosensor were optimized in terms of pH, temperature, and applied potential. The dynamic range of NO analysis was from 1.0 to 40 μM with the detection limit of 4.3 ± 0.2 nM. The reliability of biosensor was examined for the determination of NO released from the real samples of rat liver, stomach (AGS), and intestinal (HT-29) cancer cells.

1. Introduction

Nitric oxide (NO) is a free radical molecule generated in biological systems by nitric oxide synthases (NOS). It is an important messenger molecule involved in many physiological and pathological processes within the mammalian body both beneficial and detrimental (Parker, 1996). On the other hand, a deficiency of NO may play a role in some serious diseases, such as Parkinson's and Alzheimer's diseases, and an increase of NO may be a factor in some other diseases including cancer (Bredt, 1999; Christopherson and Bredt, 1997). Thus, the determination of NO has received much attention as an essential requirement ever since. However, the quantification of NO is difficult because the free radical NO has spontaneous chemical reactivity with a half-life of a few seconds (Wink and Mitchell, 1998). Therefore, various methods (Taha, 2003) have been developed for the detection of NO, such as UV–vis spectroscopy, electron spin resonance spectroscopy, chemiluminescence, fluorescence, and electrochemical methods.

Of these methods, electrochemical techniques are the most promising because they are simple, fast, sensitive, stable, and easy to fabricate with growing interest in the direct and *in vivo* measurement of NO (Isik et al., 2004; Lee et al., 2004; de Groot et al., 2005; Koh et al., 2008). Due to the redox behavior of NO molecule, it can be detected electrochemically via electrooxidation (Friedemann et al., 1996) or electroreduction (Maskus et al., 1996) that are based on the fact that NO interconvert among many species, such as nitroxyl anion, NO, and nitrosonium cation (Stamler et al., 1992). However, detection of NO based on electrooxidation generally suffered from the interferences of the oxidizing species which might co-exist during NO detection (Wu et al., 2002; Wang et al., 2005a,b; Du et al., 2008). Therefore, the measurement of NO based on electroreduction is more favorable since it can avoid interference from oxidized species. To study electroreduction of NO, various studies have been achieved using heme proteins, such as Hb and cytochrome c (Cyt c) (Koh et al., 2008; Wang et al., 2007; Haruyama et al., 1998). Microperoxidase (MP) is a small redox oligopeptide obtained by tryptic digestion of horse heart Cyt c (Tsou, 1951). It consists of eleven amino acids with a covalently linked Fe III-protoporphyrin IX heme site. Because of its simplicity and small size (Moore et al., 1996), MP has been used as a peroxidase for the fabrication of H_2O_2 biosensors (Wang et al., 2005a,b; Zhu et al., 2007). So far, there have been no reports concerning the direct application of MP for the electrochemical measurement of NO. Due to the presence of heme group in the MP molecule, it can be used as a sensing element for the electrochemical reduction of NO to fabricate a highly sensitive NO biosensor.

* Corresponding author. Tel.: +82 51 510 2244; fax: +82 51 514 2430.
E-mail address: ybshim@pusan.ac.kr (Y.-B. Shim).

0956-5663/$ – see front matter © 2010 Elsevier B.V. All rights reserved.
doi:10.1016/j.bios.2010.08.070

However, the significant challenge in the electrochemical reduction of NO in biological systems is the presence of the interferences of reduced species (H_2O_2 and O_2^-). Thus, the electrode surface is usually modified with layers of Nafion to avoid the interferences from these species. However, a disadvantage of this method is the loss of sensitivity of the biosensor surface towards NO detection by these layers (Koh et al., 2008; Wang et al., 2005a,b). Thus, co-immobilizing catalase (CAS) and superoxide dismutase (SOD) in a three-enzyme system for NO detection can completely prevent the interferences of H_2O_2 and O_2^-, as well as retain the enzyme bioactivity by providing a biological environment. To our knowledge, the electrochemical detection of NO using a three-enzyme system together with MP is being reported for the first time.

Conducting polymers have attracted much attention due to their conducting nature and biocompatibility that makes these materials excellent matrices for immobilizing biomolecules to develop a wide variety of biosensors and immunosensors (Ban et al., 2004; Kwon et al., 2006; Rahman et al., 2008). On the other hand, carbon nanotubes (CNT) have received considerable interest over the past decade due to their unique characteristics, such as high electrical conductivity, high chemical stability, and high mechanical strength with modulus (Iijima, 1991; Ajayan, 1999). The composite films of CNT with conducting polymers have recently been employed for enhancing the electrical conductivity and chemical properties of the polymer film, such as polyaniline, and polypyrrole (Cochet et al., 2001; Chen et al., 2000). The CNT composite, with the conductive polymer having functional groups, can be used as an immobilizing matrix for biomolecules to enhance sensing performances by facilitating the electron transfer reactions between biomolecules and the electrode surface.

In the present study, a highly sensitive and selective electrochemical method for NO detection was achieved by covalently immobilizing three enzymes including MP, catalase (CAS), and superoxide dismutase (SOD) onto the MWCNT-poly-5,2′:5′,2″-terthiophene-3′-carboxylic acid (PTTCA) nanocomposite layer. In this system, MP was used as a catalyst for the reduction of NO, while CAS and SOD were used to prevent the interferences of H_2O_2 and O_2^- during the electrochemical reduction of NO. The CAS/SOD/MP/MWCNT-PTTCA/AuNPs probe was characterized using scanning electron microscopy (SEM), X-ray photoelectron spectroscopy (XPS), and quartz crystal microbalance (QCM). The experimental parameters which affect the biosensor response, such as pH, temperature, and applied potential were optimized. Interference effects from other biological compounds were also investigated. To evaluate the performance of the surface probe, an experiment was conducted for the determination of NO release from rat liver and cancer cells.

2. Experimental

2.1. Materials

Microperoxidase (MP), catalase (CAS), 1-ethyl-3(3-(dimethylamino)-propyl)carbodiimide (EDC), N-hydroxysuccinimide (NHS), dichloromethane (99.8%, anhydrous, sealed under N_2 gas), $HAuCl_4$, H_2O_2, ascorbic acid (AA), glutamic acid (Glu), potassium supeoxide (KO_2), and L-arginine (L-Arg) were purchased from Sigma (USA). Bovine erythrocyte superoxide dismutase (SOD) was purchased from Calbiochem (UK). Multi-wall carbon nanotube (MWCNT) with average diameter varies from 4 to 12 nm and 99% purity, was purchased from Iljin Nanotech (South Korea). Tetrabutylammonium perchlorate (TBAP) was received from Fluka (USA), purified and dried under a vacuum. A 5,2′:5′,2″-terthiophene-3-carboxylic acid (TTCA) was synthesized according to a previous report (Lee and Shim, 2001). All other chemicals were of extra pure analytical grade and used without further purification. All aqueous solutions were prepared in doubly distilled water, which was obtained from a Milli-Q water purifying system (18 MΩ cm). Nitrogen gas (99.99%) was used for maintaining deoxygenation in the measurement cell solution before and during the experiments.

2.2. Preparation of NO and O_2^- solutions

The NO solution of 1.9 mM was prepared by bubbling 8 ml of an oxygen-free 0.1 M phosphate buffer solution (pH 7.0) with NO gas (99.99%) for about 20 min (Koh et al., 2008). A 10 mM solution of O_2^- was obtained by dissolving KO_2 in a mixture solution of dimethyl sulfoxide (DMSO) and a 0.1 M (pH 7.0) of phosphate buffer (4:1) (Kwon et al., 2006). The NO and O_2^- solutions were prepared at room temperature 25 °C and stored at 4 °C until use.

2.3. Rat liver sample

The rat liver real sample was prepared according to the following procedure; at first, the liver was removed from the rat and washed with the sterile isolating medium (0.25 mol/l sucrose, 1.0 mmol/l EDTA, 10 mmol/l Tris with pH buffered to 7.4, using HCl). Then, the liver was homogenized, and centrifuged at 4000 rpm for 15 min. The clear supernatant was centrifuged again for 15 min at 4000 rpm. The liquid was then centrifuged twice at 10,000 rpm for 15 min each time. This was resuspended in the isolating medium to give 4.8 mg/ml protein concentration, which was determined using UV spectrophotometry.

2.4. Cell culture sample

Gastric adenocarcinoma (AGS) and colon adenocarcinoma (HT-29) cells (American Type Culture Collection, anassas, VA) were cultured in Dulbecco's Modified Eagle's Medium (Gibco), supplemented with 15% fetal calf serum (Gibco), 0.1 mM mercaptoethanol (Sigma), 0.1 mM non-essential amino acids (Gibco), 100 U/ml penicillin, and 100 mg/ml streptomycin (Gibco). Briefly, cells were trypsinized and suspended in 10 ml of differentiation medium (Iscove's Modified Dulbecco's Media), 15% FBS, 2.0 mM L-glutamine, 0.1 mM non-essential amino acids, 100 U/ml penicillin, 100 mg/ml streptomycin and cultured in 100 mm non-adhesive Petri dishes to allow cells to aggregate and form embryoid bodies (EBs). Cells were placed on 0.1% gelatin coated Petri dishes and medium was replaced every 2 days.

2.5. Instruments

Cyclic voltammograms and chronoamperograms were recorded using a Potentiostat/Galvanostat, Kosentech model PT-1 (Busan, South Korea). Quartz crystal microbalance (QCM) experiments were performed using a Seiko EG&G model QCA 917 and a PAR model 263A potentiostat/galvanostat. An Au working electrode (area, 0.196 cm^2; 9 MHz; AT-cut quartz crystal) was used for the QCM experiment. XPS experiments were performed using a VG scientific ESCA lab 250 XPS spectrometer coupled with a monochromated Al Kα source having charge compensation, and SEM images were obtained using a Cambridge Stereoscan 240, at the Korea Basic Science Institute (Busan, South Korea). The CAS/SOD/MP/MWCNT-PTTCA/AuNPs/GCE probe with area of 0.07 cm^2 was used as a working electrode. Ag/AgCl and platinum wire were used as reference and counter electrodes, respectively.

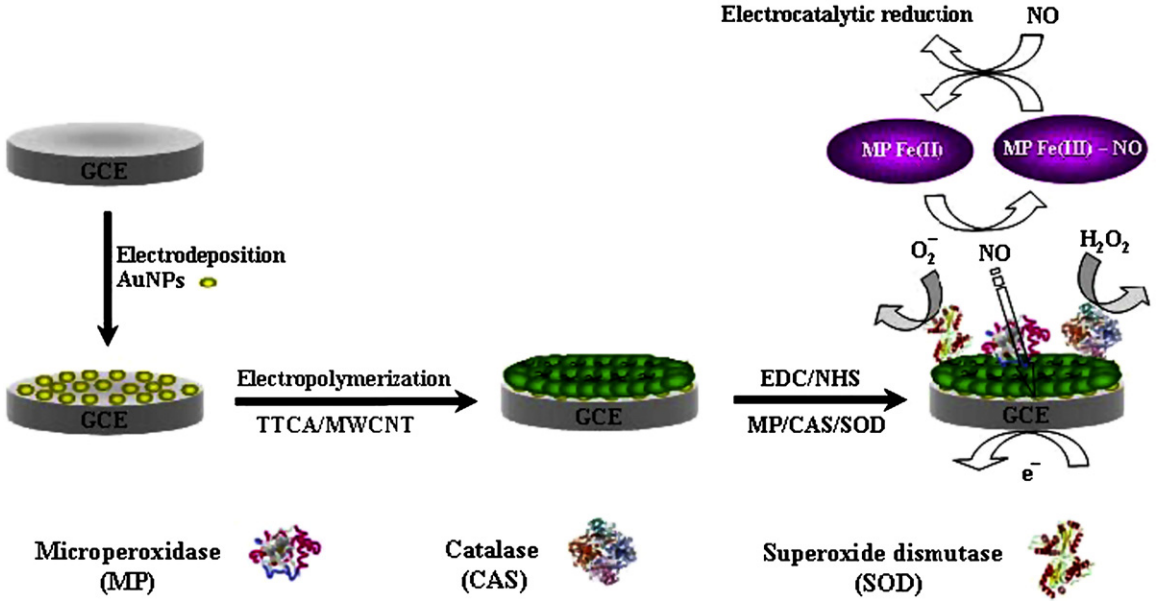

Scheme 1. Schematics for the overall detection process of NO with the CAS/SOD/MP/MWCNT-PTTCA/AuNPs biosensor.

2.6. Functionalization of MWCNT

The MWCNT was functionalized by acid treatment according to the following procedure. Firstly, a 50 ml of a mixture solution from concentrated HNO_3 and H_2SO_4 (1:3) containing 50 mg of MWCNT was sonicated for about 8 h. Thereafter, the mixture was washed with distilled water and filtrated for several times using the filter membrane (0.2 μm) until the pH of the filtrates became neutral. Then, the precipitate was dried in the oven at 80 °C for about 12 h. This process produces the carboxylated MWCNT, and therefore it can be used as a matrix for covalent immobilizing biomolecules. Finally, the carboxylated MWCNT was stored at room temperature until use.

2.7. Preparation of the MWCNT-PTTCA nanocomposite

Prior to the modification, the glassy carbon electrode (GCE) was polished with 0.5 μm alumina slurry on an emery paper to a mirror finish, and then rinsed with doubly distilled water. AuNPs were electrodeposited on GCE by linear sweep voltammetry from +1.5 to +0.5 V in 0.5 M H_2SO_4 solution containing 0.25 mM $HAuCl_4$. The size of deposited AuNPs was determined to be about 20 nm with SEM (Shiddiky et al., 2001). Thereafter, 1.0 mg/ml of carboxylated MWCNT was added to a 0.1 M TBAP/CH_2Cl_2 solution containing the 1.0 mM TTCA monomer and sonicated the solution for about 30 min. The MWCNT-PTTCA nanocomposite layer was formed by cycling the potential from 0 to +1.6 V in the mixture solution containing carboxylated MWCNT and TTCA monomer for three cycles at the scan rate of 0.1 V/s. Then, the MWCNT-PTTCA nanocomposite coated electrode was washed with CH_2Cl_2 to remove the excess mixture solution.

2.8. Immobilization of MP, SOD, and CAS onto the MWCNT-PTTCA nanocomposite layer

For the fabrication of the sensor probe, the MWCNT-PTTCA/AuNPs coated electrode was immersed for 3 h in a 0.1 M phosphate buffer solution (pH 7.0) containing a mixture of 10 mM EDC/NHS to activate the carboxylic acid groups of the MWCNT-PTTCA layer. Thereafter, the EDC-treated MWCNT-PTTCA/AuNPs electrode was washed with a phosphate buffer solution (pH 7.0). For MP, SOD, and CAS immobilization, the EDC-treated MWCNT-PTTCA/AuNPs electrode was separately incubated in 1.0 mg/ml of MP, 1.0 mg/ml of SOD, and 1.0 mg/ml of CAS solutions for 6 h. The enzymes (MP, SOD, and CAS) were immobilized onto the MWCNT-PTTCA/AuNPs layer through the formation of covalent bonds between the carboxylic acid groups of the nanocomposite (MWCNT-PTTCA) and the amine groups of the enzymes. Then, the CAS/SOD/MP/MWCNT-PTTCA/AuNPs surface was washed with a 0.1 M phosphate buffer solution (pH 7.0) and stored at 4 °C until use. The schematic of the biosensor fabrication is presented in Scheme 1.

3. Results and discussion

3.1. Characterization of the CAS/SOD/MP/MWCNT-PTTCA layer

Fig. 1A shows the SEM images for (i) AuNPs/GC; (ii) PTTCA/AuNPs/GC; (iii) MWCNT-PTTCA/AuNPs/GC; and (iv) CAS/SOD/MP/MWCNT-PTTCA/AuNPs/GC. As shown, the image of the AuNPs/GC layer shows the formation of AuNPs with a particle size of about 20 nm. The morphology of the MWCNT-PTTCA/AuNPs layer shows a homogeneous nanocomposite of MWCNT and PTTCA, while the nanocomposite film was not observed when the SEM image was obtained for the PTTCA/AuNPs layer. This indicates that the formation of the nanocomposite layer of MWCNT-PTTCA might be due to the incorporation of MWCNT into PTTCA during the electropolymerization process. The diameter of MWCNT in the nanocomposite film was determined to be about 10 nm. Moreover, the SEM image obtained for the CAS/SOD/MP/MWCNT-PTTCA/AuNPs/GC layer shows a different structure with large clusters from that obtained for the MWCNT-PTTCA/AuNPs/GC, suggesting that CAS, SOD, and MP were immobilized on MWCNT-PTTCA layer.

The bond formation during immobilization of CAS, SOD, and MP on the MWCNT-PTTCA nanocomposite layer was also investigated with XPS. All XPS spectra were taken after Ar ion gas etching for 50 s and corrected using a C1s peak at 284.6 eV as an internal standard. Fig. 1B shows the XPS survey spectra obtained for (i) MWCNT-PTTCA/AuNP/GC, (ii) MP/MWCNT-PTTCA/AuNPs/GC, (iii) SOD/MP/MWCNT-PTTCA/AuNPs/GC, and (iv) CAS/SOD/MP/MWCNT-PTTCA/AuNPs/GC. The survey spectrum recorded for the MWCNT-PTTCA/AuNPs/GC layer showed two

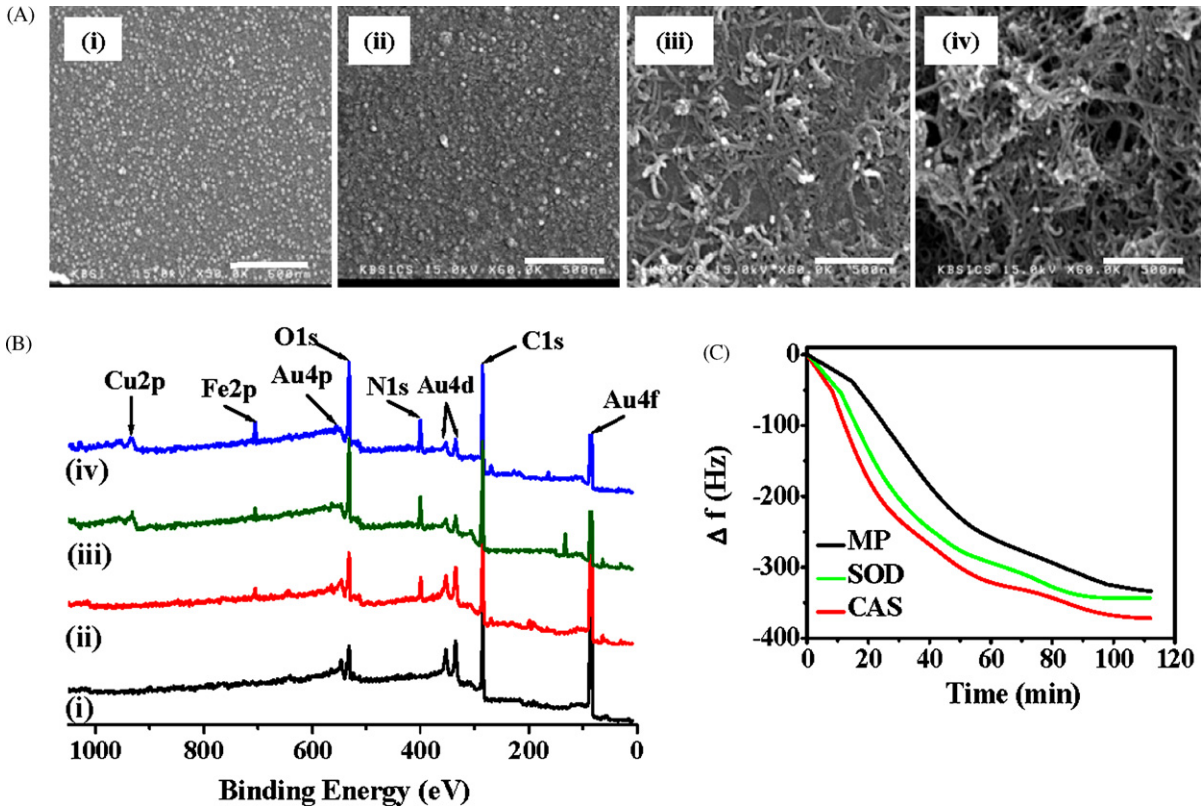

Fig. 1. (A) SEM images of (i) AuNPs/GC, (ii) PTTCA/AuNPs/GC, (iii) MWCNT-PTTCA/AuNPs/GC, and (iv) CAS/SOD/MP/MWCNT-PTTCA/AuNPs/GC layers. (B) XPS surveys of (i) MWCNT-TTCA/AuNPs/GC (black line), (ii) MP/MWCNT-PTTCA/AuNPs/GC (red line), (iii) SOD/MP/MWCNT-PTTCA/AuNPs/GC (green line) and (iv) CAS/SOD/MP/MWCNT-PTTCA/AuNPs/GC (blue line) layers. (C) QCM analysis during the immobilization of MP (black line), SOD (green line), and CAS (red line). (For interpretation of the references to colour in this figure legend, the reader is referred to the web version of the article.)

peaks at 83.5 and 87.3 eV, which were related to Au4f7 and Au4f5 orbitals, respectively. Moreover, Au4d5, Au4d3, and Au4p3 peaks were observed at 334.5, 352.2, and 546.1 eV (Kwon et al., 2006). A spectrum obtained for the MP/MWCNT-PTTCA/AuNPs/GC layer showed N1s and Fe2p peaks at 400.3 and 709.1 eV. The appearing of N1s peak was due to the amide bond formation between the amine of MP and carboxylic acid groups of the nanocomposite (MWCNT-PTTCA). The Fe2p peak observed at 709.1 eV was related to the Fe ion in the heme group of MP. Subsequently, the XPS survey spectra obtained for the SOD/MP/MWCNT-PTTCA/AuNPs/GC layer show an additional peak of Cu2p at 930.9 eV, which originated from Cu of the SOD. Furthermore, the spectra obtained after the immobilization of CAS show an increase in the peak signal at 709.1 eV which related to the Fe ion in the heme group of CAS. XPS results indicated that these three enzymes were successfully immobilized on the nanocomposite layer of MWCNT-PTTCA.

Further studies were performed through QCM experiments to estimate the amount of each enzyme immobilized on the MWCNT-PTTCA layer based on the frequency change. The mass of the enzymes immobilized on the electrode surface was calculated using an equation previously reported (Lee and Shim, 2001). Fig. 1C shows the plots of frequency according to the time obtained during the immobilization of MP (black line), SOD (green line), and CAS (red line) onto the MWCNT-PTTCA layer. The frequency decreased upon the immobilization of MP on the MWCNT-PTTCA layer and reached a steady state after about 2 h with a 333 ± 5 Hz frequency shift, indicating that the immobilization of MP was completed after about 2 h. For the immobilization of SOD on the MP/MWCNT-PTTCA layer, a steady stated was observed after about 2 h and the frequency shift was 341 ± 3 Hz. During the immobilization of CAS onto the SOD/MP/MWCNT-PTTCA layer, a steady state was attained after about 2 h, where a 374 ± 7 Hz frequency shift was observed. The amounts of MP, SOD, and CAS immobilized onto the MWCNT-PTTCA layer were estimated to be 0.07, 0.08, and 0.36 μg, which corresponded to 2.2×10^{-11}, 2.3×10^{-12}, and 3.2×10^{-13} mol/cm^2, respectively.

3.2. Direct electrochemistry of immobilized CAS, SOD, and MP on the MWCNT-PTTCA/AuNPs layer

Fig. 2A shows the CVs recorded for the CAS/SOD/MP/MWCNT-PTTCA/AuNPs (red-solid line), MWCNT-PTTCA/AuNPs (black-dashed line), SOD/MWCNT-PTTCA/AuNPs (gray-solid line), MP/MWCNT-PTTCA/AuNPs (blue-solid line), and CAS/MWCNT-PTTCA/AuNPs (green-solid line) layers in a 0.1 mM phosphate buffer solution of pH 7.0. Three well-defined redox peaks were observed at −0.11/+0.05, −0.33/−0.28, and −0.46/−0.41 V vs. Ag/AgCl for the SOD/MWCNT-PTTCA/AuNPs, MP/MWCNT-PTTCA/AuNPs, and CAS/MWCNT-PTTCA/AuNPs layers, respectively. These three redox peaks were simultaneously observed at −0.11/+0.04, −0.33/−0.27, and −0.47/−0.40 V vs. Ag/AgCl for the CAS/SOD/MP/MWCNT-PTTCA/AuNPs layer, which indicated that the three enzymes (CAS, SOD, and MP) were successfully co-immobilized on the MWCNT-PTTCA/AuNPs layer. However, no redox peaks were observed when the CV was recorded for the MWCNT-PTTCA/AuNPs layer. This indicates that these redox peaks were related to the immobilized SOD, MP, and CAS on the MWCNT-PTTCA/AuNPs layer, which might be due to the direct electron transfer processes of Cu(I)/Cu(II), Fe(II)/Fe(III), and Fe(II)/Fe(III) redox centers in the enzymes, respectively. The redox peak currents of CAS, MP, and SOD were directly proportional to the scan rate, indicating that the electrode reactions were involved in the surface confined processes through the direct electron transfer reaction. The peak separations of the redox couples increased with

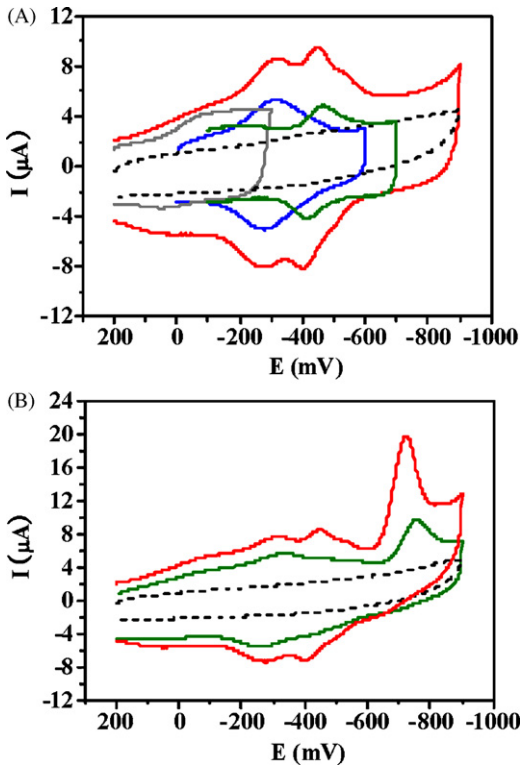

Fig. 2. (A) CVs recorded for MWCNT-PTTCA/AuNPs (black-dashed line), SOD/MWCNT-PTTCA/AuNPs (gray-solid line), MP/MWCNT-PTTCA/AuNPs (blue-solid line), CAS/MWCNT-PTTCA/AuNPs (green-solid line), and CAS/SOD/MP/MWCNT-PTTCA/AuNPs (red-solid line) layers in a 0.1 M PBS (pH 7.0). (B) CVs recorded for a MWCNT-PTTCA/AuNPs (black-dashed line), CAS/SOD/MP/PTTCA/AuNPs (green-solid line), and CAS/SOD/MP/MWCNT-PTTCA/AuNPs (red-solid line) layers in a 0.1 M PBS (pH 7.0) containing 20.0 μM of NO. (For interpretation of the references to colour in this figure legend, the reader is referred to the web version of the article.)

the increase of the scan rate, indicating that the redox reactions were quasi-reversible. The electron transfer rate constants (k_s) were determined using the Laviron equation (Laviron, 1979):

$$\log k_s = \alpha \log(1-\alpha) + (1-\alpha)\log\alpha - \log\frac{RT}{nF\nu} - \frac{\alpha(1-\alpha)nF\,\Delta E_p}{2.3RT}$$

where n is the number of electrons transferred; F is the Faraday constant; R is the gas constant; T is the absolute temperature; ν is the scan rate; and α is the charge transfer coefficient which was estimated to be 0.45. The values of k_s were calculated to be 1.27, 1.31 and 0.48 s^{-1} at the scan rate of 0.05 V/s for CAS, MP, and SOD, respectively (Laviron, 1979).

3.3. Electrocatalytic reduction of NO on the CAS/SOD/MP/MWCNT-PTTCA/AuNPs probe

Fig. 2B shows the CVs recorded for MWCNT-PTTCA/AuNPs (black-dashed line), CAS/SOD/MP/PTTCA/AuNPs (green-solid line), and CAS/SOD/MP/MWCNT-PTTCA/AuNPs (red-solid line) layers in a 0.1 M phosphate buffer solution (pH 7.0) containing 20.0 μM NO. As seen, no peak was observed when the CV was recorded for the MWCNT-PTTCA/AuNPs electrode. However, a cathodic peak was observed at −0.75 V with the CAS/SOD/MP/PTTCA/AuNPs electrode, which attributed to the catalytic function of the immobilized MP on the PTTCA layer. The reduction peak of NO which was observed using MP is close to that observed using hemoglobin modified electrode (Koh et al., 2008). This indicated that the reduction process of NO is greatly facilitated by MP. The reduction peak of NO was largely increased when the CV was recorded for the MWCNT composite probe (CAS/SOD/MP/MWCNT-PTTCA/AuNPs) (Scheme 1). This result provides evidence that the use of MWCNT-PTTCA nanocomposite layer as a matrix significantly enhanced the efficiency of immobilized enzymes to promote their direct electron transfer processes and hence resulted in the higher catalytic response for the reduction of NO. Therefore, the subsequent study for NO detection was performed for the CAS/SOD/MP/MWCNT-PTTCA/AuNPs probe.

3.4. Optimization of the experimental parameters for NO detection

Experimental parameters that affect the electrocatalytic reduction of NO were optimized in terms of pH, temperature, and the applied potential. The effect of pH on the catalytic reduction of NO with the CAS/SOD/MP/MWCNT-PTTCA/AuNPs electrode was investigated in the range from pH 2.0 to 8.0. As shown in Fig. 3A, the current response of NO increased with increasing pH from 2.0 to 4.0. Thereafter, the current response significantly decreased when the pH increased to 8.0. Thus, the optimum pH for NO detection was chosen to be pH 4.0.

The temperature dependency of the catalytic reduction of NO was also examined from 10 to 50 °C (Fig. 3B). The current increased as the temperature increased from 10 to 25 °C and it decreased when the temperature increased further. This might be because the biological activity of the immobilized enzymes on the MWCNT-PTTCA/AuNPs layer decreased at high temperatures. Thus, 25 °C was chosen to be as the optimal temperature.

The effect of applied potential on the amperometric current response of NO was studied for the CAS/SOD/MP/MWCNT-PTTCA/AuNPs electrode (Fig. 3C). The response increased as the applied potential went from −0.1 to −0.8 V, while applying the more negative potential (up to −1.1 V) did not significantly affect the response. Hence, −0.8 V was used as the optimum applied potential for the chronoamperometric measurements of NO.

3.5. Amperometric response of the NO biosensor

Fig. 4A shows the typical current–time response upon varying concentrations of NO in the buffer solution (pH 4.0). The increase in the catalytic responses was observed after every injection of NO. The biosensor showed a linear relationship at the NO concentration range from 1.0 to 40 μM. The linear regression equation was expressed as: I_p (μA) = 1.65 (±0.2) + 1.20 (±0.01) [NO] (μM), with the correlation coefficient of 0.999. The relative standard deviation (RSD) was determined to be 1.7% and the detection limit was determined to be 4.3 ± 0.2 nM based on five measurements of the standard deviation of the blank noise (95% confidence level, k = 3, n = 5). The sensitivity of the NO biosensor was 1.10 ± 0.01 μA/μM with a response time of 3.60 ± 0.03 s/μM. The lower detection limit of the proposed biosensor as compared with other reported NO biosensors (Koh et al., 2008; Pang et al., 2003; Topoglidis et al., 2003; Wu et al., 2002; Wang et al., 2005a,b; Friedemann et al., 1996; Malinski and Taha, 1992; Jia et al., 2009) suggested that the biosensor developed in this study might be efficient for NO detection in biological samples.

3.6. Interference effect

In order to investigate the selectivity of the CAS/SOD/MP/MWCNT-PTTCA/AuNPs probe for NO detection, the amperogram of 2.0 μM NO and other biological interfering species in their physiological level, such as 10 μM H_2O_2, 10 μM O_2^-, 1.0 mM AA, 1.0 mM L-Arg, and 1.0 mM Glu was recorded (Fig. 4B). As shown, these species did not interfere during detection of NO, even H_2O_2 and O_2^-, which are the most interfering species for NO detection at this particular potential. This indicates

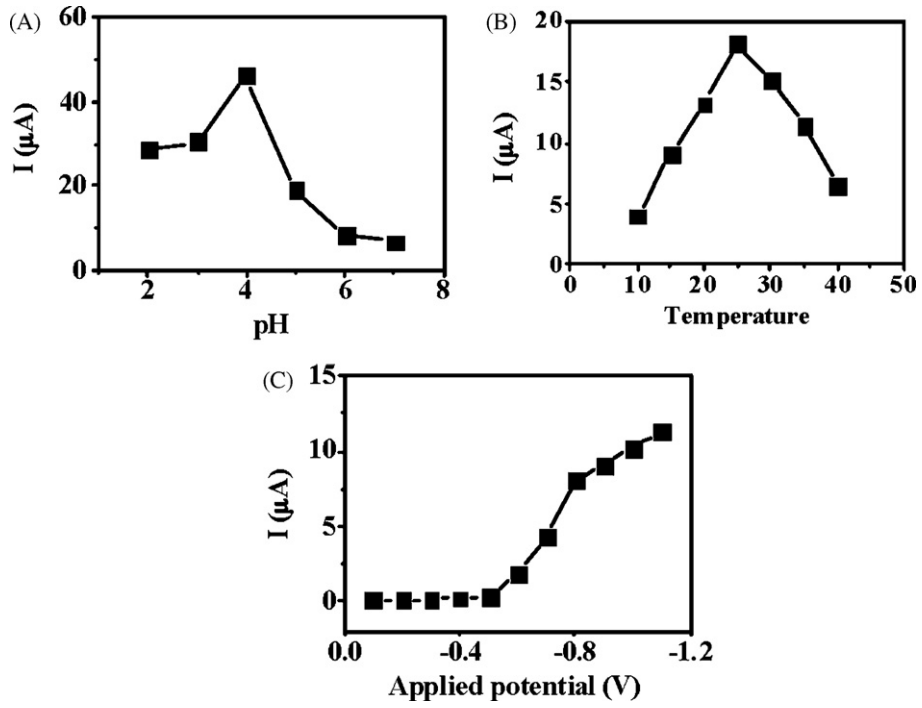

Fig. 3. Optimizations of experimental conditions of the NO biosensor with the CAS/SOD/MP/MWCNT-PTTCA/AuNPs probe; (a) pH, (b) temperature, and (c) applied potential.

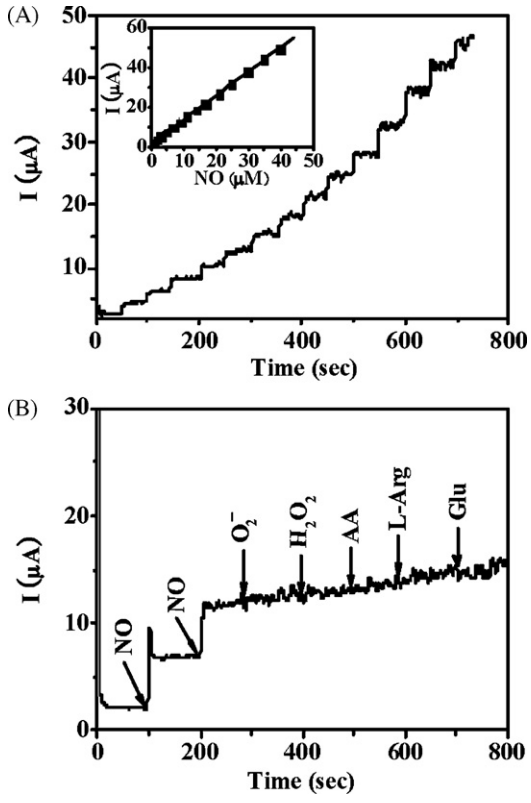

Fig. 4. (A) Amperometric response recorded for the CAS/SOD/MP/MWCNT-PTTCA/AuNPs probe upon the addition of NO in a buffer solution (pH 4.0). Inset shows the corresponding calibration plot. (B) Amperometric response recorded during injection of 2.0 μM NO and other interfering compounds in their physiological level, such as 10 μM H_2O_2, 10 μM O_2^-, 1.0 mM AA, 1.0 mM L-arginine (L-Arg), and 1.0 mM glutamic acid (Glu).

that the immobilized CAS and SOD on the MWCNT-PTTCA/AuNPs layer completely eliminated the interferences of H_2O_2 and O_2^- during NO detection as shown in Scheme 1. The results show that the present biosensor enables the selective detection of NO in the presence of interfering compounds without losing any of its sensitivity.

3.7. Stability of the NO biosensor

To investigate the long-time stability of the proposed biosensor, the response of CAS/SOD/MP/MWCNT-PTTCA/AuNPs probe towards NO was recorded with respect to the storage time, during which the biosensor was examined three times in an every week. The biosensor retained about 97% of its initial response to the reduction of NO over a period of one month. However, the sensitivity slightly decreased after one month which might have been occurred due to the loss of the enzymes from the probe surface. In the same direction, the stability of the biosensor to multiple uses was also investigated. The biosensor lost only about 2.5% from its initial response to NO after 20 continuous measurements. Moreover, the sensor-to-sensor variation has been investigated for 5 electrodes and there was no significant difference between their responses. These results suggested that the proposed NO biosensor has long-time stability and can be used over one month without significant change in its response to NO.

3.8. Analytical applications

To examine the validity of the proposed biosensor for the real sample applications, the determination of NO released from the rat liver as well as cultured cells (human stomach (AGS) and intestinal (HT-29) cancer cells) was studied. NO is generally generated in biological systems through the interaction of NOS with L-Arg (Moncada et al., 1991). Thus, it is expected that mixing the real samples (rat liver, AGS, and HT-29 cells) with L-Arg could produce NO. Our preliminary experiments indicated that the addition of real samples into the buffer solution (pH 4.0) in the absence of L-Arg did not show any response to NO. Thus, the detection of the real samples

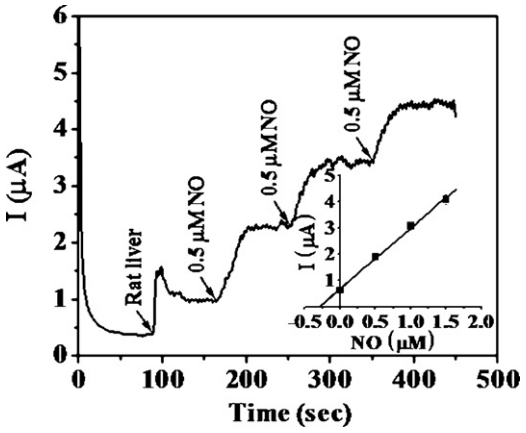

Fig. 5. Amperometric response recorded during the standard addition of NO released from rat liver in the buffer solution containing 1.0 mM L-Arg. Inset showed the corresponding standard addition plot.

was performed in the presence of 1.0 mM L-Arg. Hence, NO released from this reaction can be detected using the CAS/SOD/MP/MWCNT-PTTCA/AuNPs biosensor.

Fig. 5 shows the amperogram recorded during the addition of a 1.0 ml of rat liver sample in a 9.0 ml buffer solution (pH 4.0) containing 1.0 mM L-Arg, followed by adding different concentrations of a standard solution of NO. Inset of Fig. 5 shows the corresponding standard addition plot. The linear regression equation was expressed as: I_p (μA) = 0.63 (±0.03) + 2.40 (±0.09) [NO] (μM), with the correlation coefficient of 0.996 and the relative standard deviation (RSD) was determined to be 0.83. The average concentration of NO released from rat liver sample ($n = 3$) was determined to be 3.82 ± 0.83 μM. This result was comparable with that obtained for NO released from rat liver (1.3–2.5 μM) using a cyanoethyl cellulose–hemoglobin biosensor (Jia et al., 2009).

In order to evaluate the accuracy of this method, the quantity of NO released from stomach (AGS) and intestinal (HT-29) cancer cells was also estimated according to the above procedures. Typical amperometric responses of NO released from 57×10^3 AGS cells and 75×10^3 HT-29 cells are also observed using standard addition plots (figure not shown). The linear regression equations of the calibration plots for AGS and HT-29 were expressed as: I_p (μA) = 0.56 (±0.02) + 1.75 (±0.07) [NO] (μM), and I_p (μA) = 0.83 (±0.04) + 2.17 (±0.10) [NO] (μM), with the correlation coefficient of 0.994 and 0.999, and the relative standard deviation (RSD) were determined to be 0.27 and 0.67, respectively. The average concentrations of NO released from AGS and HT-29 cell samples ($n = 3$) were determined to be 3.91 ± 0.27 and 4.42 ± 0.67 μM, respectively. These values are in agreement with that reported previously for *in vivo* measurements of NO (1.3–6.3 μM) (Malinski, 2002), which strongly suggested that the proposed biosensor can be used for real detection of NO in biological systems.

4. Conclusions

A NO biosensor based on a three-enzyme system (MP, CAS, and SOD) immobilized at the MWCNT-PTTCA nanocomposite layer was successfully fabricated. The use of the MWCNT-PTTCA nanocomposite layer as a matrix provides a large surface area for sufficient amounts of immobilized enzymes through the covalent bond formation. The biosensor exhibited an excellent catalytic response towards the electrochemical reduction of NO having a wide linear range between 1.0 and 40 μM with a detection limit of 4.3 ± 0.2 nM. The application of the proposed biosensor was successfully performed to determine NO released from rat liver, AGS, and HT-29 samples. The stable, sensitive, and specific response to NO indicates that the CAS/SOD/MP/MWCNT-PTTCA/AuNPs biosensor is an excellent method for NO detection and it can be used for biological samples effectively.

Acknowledgement

This research was supported by the Korea Ministry of Environment as "The Eco-Technopia 21 Project" (Grant No. 091-082-078).

References

Ajayan, P.M., 1999. Chem. Rev. 99, 1787–1800.
Ban, C., Chung, S., Park, D.S., Shim, Y.-B., 2004. Nucleic Acids Res. 32, e110.1–e110.8.
Bredt, D.S., 1999. Free Radical Res. 31, 577–596.
Chen, G.Z., Shaffer, M.S.P., Coleby, D., Dixon, G., Zhou, W., Fray, D.J., Windle, A.H., 2000. Adv. Mater. 12, 522–526.
Christopherson, K.S., Bredt, D.S., 1997. J. Clin. Invest. 100, 2424–2429.
Cochet, M., Maser, W.K., Benito, A.M., Callejas, M.A., Martinez, M.T., Benoit, J.-M., Schreiber, J., Chauvet, O., 2001. Chem. Commun., 1450–1451.
de Groot, M.T., Merkx, M., Wonders, A.H., Koper, M.T.M., 2005. J. Am. Chem. Soc. 127, 7579–7586.
Du, F., Huang, W., Shi, Y., Wang, Z., Cheng, J., 2008. Biosens. Bioelectron. 24, 415–421.
Friedemann, M.N., Robinson, S.W., Gerhardt, G.A., 1996. Anal. Chem. 68, 2621–2628.
Haruyama, T., Shiino, S., Yanagida, Y., Kobatake, E., Aizawa, M., 1998. Biosens. Bioelectron. 13, 763–769.
Iijima, S., 1991. Nature 354, 56–58.
Isik, S., Etienne, M., Oni, J., Blochl, A., Reiter, S., Schuhmann, W., 2004. Anal. Chem. 76, 6389–6394.
Jia, S., Fei, J., Zhoub, J., Chena, X., Meng, J., 2009. Biosens. Bioelectron. 24, 3049–3054.
Koh, W.C.A., Rahman, M.A., Choe, E.S., Lee, D.K., Shim, Y.-B., 2008. Biosens. Bioelectron. 23, 1374–1381.
Kwon, N.-H., Rahman, M.A., Won, M.-S., Shim, Y.-B., 2006. Anal. Chem. 78, 52–60.
Laviron, E., 1979. J. Electroanal. Chem. 101, 19–28.
Lee, Y., Oh, B.K., Meyerhoff, M.E., 2004. Anal. Chem. 76, 536–544.
Lee, T.Y., Shim, Y.-B., 2001. Anal. Chem. 73, 5629–5632.
Malinski, T., 2002. In: Bard, A.J., Stratmann, M., Wilson, G.S. (Eds.), Encyclopedia of Electrochemistry (Bioelectrochemistry): Electrochemical Measurements of Nitric Oxide in Biological Systems, vol. 9. Wiley-VCH, Verlag GmbH, Weinheim.
Maskus, M., Pariente, F., Wu, Q., Toffanin, A., Shapleigh, J.P., Abruna, H.D., 1996. Anal. Chem. 68, 3128–3134.
Malinski, T., Taha, Z., 1992. Nature 358, 676–678.
Moncada, S., Palmer, R.M., Higgs, E.A., 1991. Pharm. Rev. 43, 109–142.
Moore, A.N.J., Katz, E., Willner, I., 1996. J. Electroanal. Chem. 417, 189–192.
Pang, J., Fan, C., Liu, X., Chen, T., Li, G., 2003. Biosens. Bioelectron. 19, 441–445.
Parker, L. (Ed.), 1996. Nitric Oxide, Part B. Physiological and Pathological Processes; Methods in Enzymology, vol. 269. Academic Press, San Diego, CA.
Rahman, M.A., Noh, H.-B., Shim, Y.-B., 2008. Anal. Chem. 80, 8020–8027.
Shiddiky, M.J.A., Rahman, M.A., Shim, Y.-B., 2001. Anal. Chem. 79, 3724–3733.
Stamler, J.S., Singel, D.J., Loscalzo, J., 1992. Science 258, 1898–1902.
Taha, Z.H., 2003. Talanta 61, 3–10.
Topoglidis, E., Astuti, Y., Duriaux, F., Gratzel, M., Durrant, J.R., 2003. Langmuir 19, 6894–6900.
Tsou, C.L., 1951. Biochem. J. 49, 362–367.
Wang, F., Chena, X., Xua, Y., Hua, S., Gaoa, Z., 2007. Biosens. Bioelectron. 23, 176–182.
Wang, M., Zhao, F., Liu, Y., Dong, S., 2005a. Biosens. Bioelectron. 21, 159–166.
Wang, Y.Z., Li, Q., Hu, S.S., 2005b. Bioelectrochemistry 65, 135–142.
Wink, D.A., Mitchell, J.B., 1998. Free Radical Biol. Med. 25, 434–456.
Wu, F.H., Zhao, G.C., Wei, X.W., 2002. Electrochem. Commun. 4, 690–694.
Zhu, X., Yuri, I., Gan, X., Suzuki, I., Li, G., 2007. Biosens. Bioelectron. 22, 1600–1604.